JACS Au
AN OPEN ACCESS JOURNAL OF THE AMERICAN CHEMICAL SOCIETY

pubs.acs.org/jacsau
Article

Enhanced Dynamics and Charge Transport at the Eutectic Point: A New Paradigm for the Use of Deep Eutectic Solvent Systems

Stephanie Spittle, Ibrahim Alfurayj, Benworth Bryce Hansen, Kaylie Glynn, William Brackett, Rathiesh Pandian, Clemens Burda,* and Joshua Sangoro*

Cite This: JACS Au 2023, 3, 3024−3030
Read Online

ACCESS | Metrics & More | Article Recommendations | Supporting Information

ABSTRACT: Deep eutectic solvents (DESs) are a class of versatile solvents with promise for a wide range of applications, from separation processes to electrochemical energy storage technologies. A fundamental understanding of the correlation among the structure, thermodynamics, and dynamics of these materials necessary for targeted rational design for specific applications is still nascent. Here, we employ differential scanning calorimetry (DSC), broadband dielectric spectroscopy (BDS), and femtosecond transient absorption spectroscopy (fs-TAS) to investigate the correlation among thermodynamics, dynamics, and charge transport in mixtures comprising a wide range of compositions of choline chloride (ChCl) and ethylene glycol (EG). Detailed analyses reveal that (i) the eutectic composition of this prototypical DES occurs in the 15−20 mol % ChCl in the EG range rather than the previously assumed 33 mol %, and (ii) both rotational dynamics and charge transport at the eutectic composition are enhanced in this composition range. These findings highlight the fundamental interplay between thermodynamics and dynamics in determining the properties of DESs that are relevant to many applications.

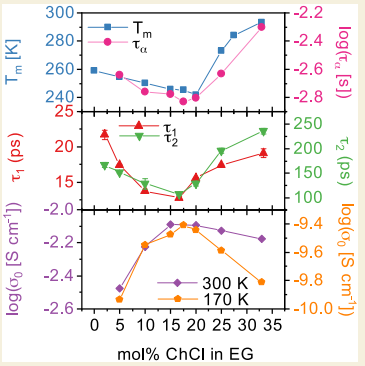

KEYWORDS: *deep eutectic solvents, solvent reorientation, solvent dynamics, eutectic composition, liquidus temperature, femtosecond dynamics, broadband dielectric spectroscopy*

INTRODUCTION

Deep eutectic solvents (DESs) are a class of solvents that have shown great potential in many areas such as biomass processing,[1−3] pharmaceutical research,[4−6] CO_2 capture,[7,8] and redox flow batteries.[9−11] The appeal for their use as alternative solvents arises from their relative ease of synthesis from potentially inexpensive and sustainable parent materials.[12,13] Many DESs are simply mixtures of two or more components that result in a depressed melting temperature significantly below that of its parent compounds.[14] The resulting properties often include wide liquidus ranges, low volatility, low flammability, and high tunability.[15−18] Since the design space for DESs is large, predictive knowledge and understanding of the impact of the chemical structure as well as composition on the physicochemical properties of the DES is important in selecting solvents for specific applications.[19] Many existing DES studies typically report properties or applications of DESs at one or two compositions, presumably due to the scarcity of data on the phase characteristics of the DES investigated. Furthermore, it has been suggested that the eutectic compositions do not necessarily matter in terms of the overall physicochemical properties of DESs, and there are no "magic" compositions.[20] While this picture may indeed hold for a limited set of properties, the general validity of this conclusion is yet to be rigorously demonstrated, especially for dynamics across multiple time scales.

Given that ethaline is one of the prototypical DESs in the current literature due to its low viscosity relative to other DESs, it is an excellent model system to employ in evaluating the potential impact of thermodynamic transitions on macroscopic dynamics.[21] Ethaline was first reported by Abbott et al. as a 1:2 molar ratio of ChCl (T_m = 575 K) to EG (T_m = 260 K) with a freezing point of 283 K.[22] However, some more recent reports have also provided conflicting values of melting temperature (T_m), such as 237[23] and 207 K.[24] Additionally, Agieienko et al. reported that the actual eutectic composition is at 17.1 mol % ChCl or a 1:4.85 molar ratio of ChCl to EG.[25] This raises pertinent questions: why are there such disparities, and how does the existence of eutectic compositions impact dynamics and charge transport in deep eutectic solvents?

In the current paper, we employ DSC, fs-TAS, and BDS to study ChCl and EG mixtures in a wide composition range to unravel the correlations between thermodynamic transitions and dynamics in these systems. We determine that the lowest liquidus temperatures occur in the 15−20 mol % ChCl range,

Received: July 28, 2023
Revised: October 18, 2023
Accepted: October 20, 2023
Published: November 7, 2023

https://doi.org/10.1021/jacsau.3c00420
JACS Au 2023, 3, 3024−3030

concomitant with the fastest dynamics measured by fs-TAS and BDS, as well as the highest dc ionic conductivity determined by BDS at the same eutectic composition. It is suggested that the enhancement of transport and dynamics at the eutectic composition is intuitive based on the well-established Lindemann's criterion qualitatively linking the melting temperatures to the glass transition. The knowledge of the range of compositions that yield eutectic systems and their impact on dynamics may prove to play a crucial role in many applications that rely on solvation in deep eutectic solvents.

RESULTS AND DISCUSSION

Figure 1 shows thermograms obtained on heating for neat EG as well as 5, 20, and 33 mol % ChCl in EG (additional compositions are included in Figure S1). These data were collected to examine the phase behavior of DESs over wide ranges of compositions and temperatures and to obtain an accurate phase diagram for ChCl/EG mixtures. Figure 1d demonstrates that EG exhibits a single melting event upon heating, typical of single-component, homogeneous systems. It is noteworthy that a corresponding cold crystallization event is not observed. As ChCl is introduced, several additional crystallization and melting events emerge, as shown in Figure 1b,c, for 20 and 5 mol % ChCl. For 33 mol % in Figure 1a, only a single broad crystallization feature is observed, followed by a broad melting feature. The broad melting event at the 33 mol % composition is an important and expected feature of eutectic mixtures.[26,27] Typically, broad melting events in DSC are attributed to a distribution of solid structures undergoing melting over a range of temperatures as opposed to the sharply defined feature for a pure, highly ordered crystal lattice such as is observed in the pure EG system.

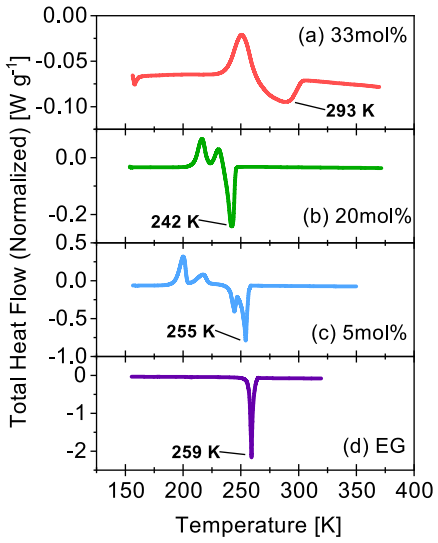

Figure 1. Temperature-modulated differential scanning calorimetry experiments for (a) 33, (b) 20, and (c) 5 mol % ChCl in EG as well as (d) neat EG. Data are displayed from heating pass of the total heat flow signal from 2 °C/min MDSC. *Y*-axis scaling of each thermogram is chosen to emphasize the liquidus transition temperatures, T_L, denoted by boldface text. Broad (a) and/or multiple melting depressions (c) are indicative of separation between solidus and liquidus temperatures, which in turn suggest that the composition is noneutectic. In this work, the error bars are smaller than the size of the symbols unless otherwise indicated.

The broad melting region for the 33 mol % ChCl is indicative of the presence of a dual-phase region in a binary phase diagram, where both solid and liquid phases are present in noneutectic compositions for a range of isotherms. These are typically denoted with solidus and liquidus transitions, where the dual-phase region is demarcated from the all-solid mixture at low temperatures and the all-liquid mixture at high temperatures, respectively. A wide dual-phase region is therefore typical of noneutectic compositions, with T_S temperatures indicating the temperature at which the solid mixture first begins to melt, and T_L the temperatures marking the final melting of all of the solid (denoted in bold).[28] We conjecture that the broad melting event of 33 mol % ChCl at around room temperature could explain numerous inconsistencies and unusual properties observed, including the ability to at least partially crystallize over extended periods of time at isotherms in the dual-phase region for this composition. Conversely, as the compositions get closer to the eutectic composition, the solidus and liquidus temperatures can converge into a single peak. When this feature also occurs at a minimum in melting temperature, said composition can be called the eutectic point of the mixture.[29] The 5 and 33 mol % compositions in Figure 1c,a demonstrate the former cases, whereas the 20 mol % demonstrates the latter case, exhibiting only a single sharp melting event at the lowest observed temperature for any of the compositions, suggesting that 20 mol % is indeed the eutectic composition for the ChCl/EG mixture. Additional calorimetric data showing additional compositions in fine mol % increments are presented in the Supporting Information (Figure S1).

The primary focus of the current work is to evaluate the correlations between the eutectic transitions and dynamics in liquid-state DESs. For many electrochemical energy conversion and storage applications, a lowered melting point at the eutectic point, corresponding to an increased ionic conductivity, ion mobility, and overall faster solvent dynamics, would be beneficial. Here, we probe solvent dynamics using transient absorption spectroscopy with a femtosecond time resolution (fs-TAS). The fs-TA technique is a well-established method to study solvent dynamics. It has been applied to over 300 solvents, and as such, the solvent response to the charge-transfer reaction of the applied probe molecule B30 is as well established as is the technique itself. Our recent work reported that the observed biexponential dynamics is due to the heterogeneous solvation environment.[32] The faster relaxation component originates with the dynamics provided by EG as the primary solvent component, while the slower component is due to the solvent environment of the dissolved choline chloride. Both components interact individually with the solvent probe B30 and are reflected in the response dynamics. In this work, we provide additional insight into the unique solvent behavior of eutectic solvent mixtures. When the solvation dynamics are measured at the concentration range around a eutectic point, the solvation dynamics become faster than when a eutectic is measured in the liquid phase far off the eutectic point. Since ChCl/EG mixtures do not absorb at visible-light wavelengths, a well-established probe for solvent relaxation dynamics, Reichhardt's dye B30, is used in this study.[30] B30 has been used for solvent studies in many prior solvent systems[30,31] and as a probe molecule recently also for deep eutectic solvents.[32]

For protic solvents such as ChCl/EG mixtures, the normalized absorbance from fs-TAS measurements decays

https://doi.org/10.1021/jacsau.3c00420
JACS Au 2023, 3, 3024−3030

with two main components that can be fitted with a biexponential function. Figure 2 shows data from two

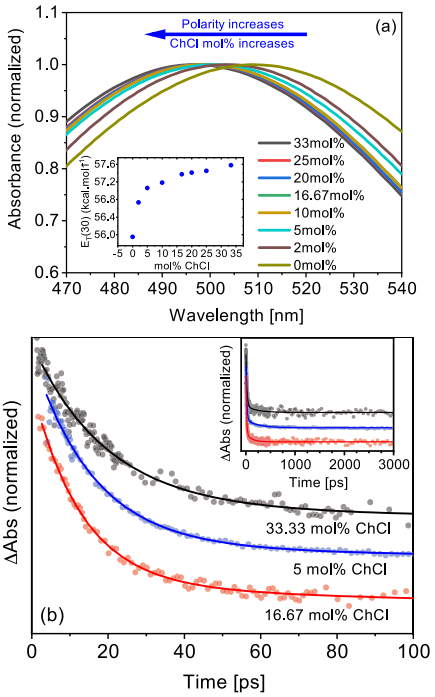

Figure 2. (a) Steady-state absorption spectra of the solvatochromic dye B30 in ethaline at various choline chloride (ChCl) concentrations from 0.0 to 33.33 mol % ChCl measured at 298 K. The continuous blue shift of λ_{max}(B30) with increasing ChCl mol % shows increasing polarity at higher mol % of ChCl. Inset: the $E_T(30)$-polarities of ethaline solutions are calculated based on their λ_{max} values as summarized in Table S2. $E_T(30)$-polarity increases with increasing the mol %. (b) fs-transient absorption kinetics of B30 measured at λ_{probe} = 580 nm at 298 K and biexponential fits at 3 different mol % of ChCl in EG. Data sets are normalized and vertically offset for direct visual comparison. Other compositions (2, 10, 20, 25 mol %) are omitted for clarity; see the SI for remaining kinetics. **Inset:** the kinetics up to 3 ns.

experiments performed with Reichardt's dye B30 (other compositions are shown in Figure S2). The first, shown in Figure 2a, displays the steady-state absorption of B30, and it is used as a measure of the solvent polarity on an accepted solvent scale of E_T30 values. The solvent polarity of ChCl/EG mixtures increases with ChCl addition, as shown in the inset. Figure 2b shows the relaxation dynamics obtained from transient absorption of B30 as a function of time for 5, 16.67, and 33.33 mol % of ChCl in EG. The spectra reveal two distinct time components, which both show that solvation dynamics are enhanced with composition up to 16.67 mol % ChCl but are slowed for 33 mol % ChCl. While there may be multiple different processes taking place in solubilizing photoexcited B30, the literature on femtosecond dynamics of B30 solvation attributes the initial fast component to the solvent reorientation while the slower component is assigned to the rearrangement of the hydrogen bonding network.[33,34] Our previous studies indicate that the slow component is consistently absent in nonprotic solvents.[35] Additional fs-TAS results for a series of ChCl/EG mixtures investigated are shown in Table S1, clearly highlighting the change in the solvation dynamics at the eutectic range, at which both time constants are the fastest.

Broadband dielectric spectroscopy was employed to study the reorientational and ion dynamics in each composition of ChCl in EG. Figure 3 shows the (a) real part of the complex

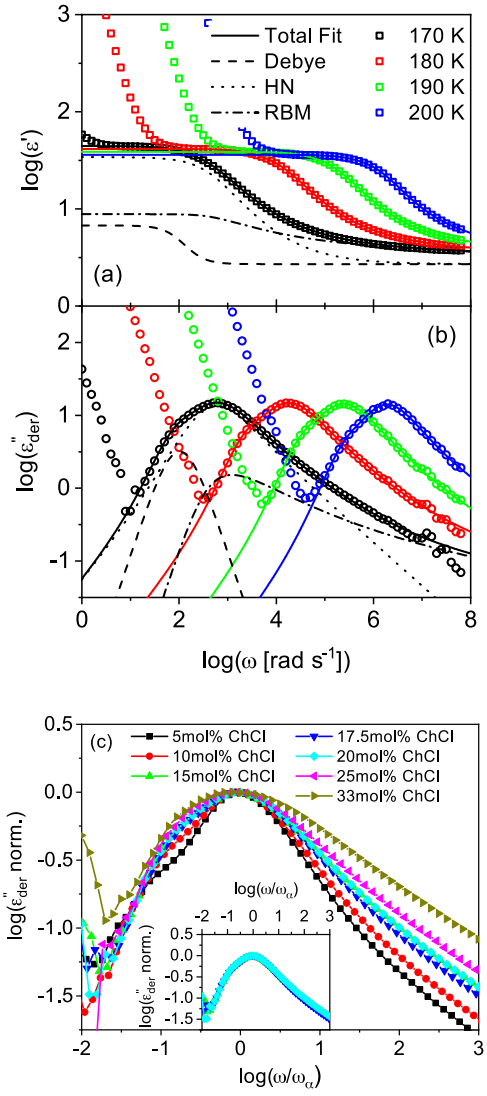

Figure 3. (a) Real part of the complex dielectric function of 20 mol % ChCl in EG at various temperatures. (b) Derivative representation of the dielectric loss for various temperatures. The solid lines are total fits, dashed lines represent the Debye function, dotted lines denote the Havriliak–Negami (HN) function, and dash-dot lines are obtained from the random barrier model (RBM), as indicated. (c) Dielectric loss obtained from the derivative representation normalized by the value at the peak of the α-relaxation plotted versus radial frequency normalized by the mean rate of the α-relaxation for each composition at 170 K. Inset: compositions of 15, 17.5, and 20 mol % ChCl isolated to show their similarity.

dielectric function as well as (b) the dielectric loss obtained from the derivative representation employed to suppress the dc ionic conductivity and reveal any underlying relaxations in the spectra of 20 mol % ChCl in EG at various temperatures. The spectra were fit with a linear combination of a Debye model, a Havriliak–Negami function, and a random barrier model (RBM) to account for ion rearrangements, structural relaxation, and ion hopping, respectively. These processes were observed for all compositions investigated, as previously reported.[36] In our previous study of ChCl/glycerol mixtures,

https://doi.org/10.1021/jacsau.3c00420
JACS Au 2023, 3, 3024–3030

we assigned the slow, Debye-like process to the rotational dynamics of choline ions that are inhibited by the hydrogen-bonded network of the hydrogen bond donor (HBD).

According to Debye's theory, relaxation of an isolated dipole can be described by an exponential function in the time domain, which yields symmetric dielectric relaxation spectra in the frequency domain.[37] Spatial and temporal inhomogeneities in a material lead to nonexponential functions, which can, in principle, be decomposed into superpositions of single exponential (Debye-like modes) functions.[38] The more heterogeneous the dynamics, the broader the distribution of local relaxation times. To evaluate the dependence of the spectral shapes on the composition of the mixtures, the dielectric loss normalized by the peak maximum is plotted versus the radial frequency, normalized by the primary structural relaxation rate for each composition, as shown in Figure 3c. As the ChCl concentration increases, the relaxation attributed to ion rearrangements speeds up and becomes more intense relative to the structural relaxation. Additionally, the spectral shapes become broader, suggesting that the mixtures are becoming more heterogeneous. This is consistent with a previous study of 33 mol % ChCl in EG, which confirmed the presence of dynamic heterogeneities.[39] The similarity of the spectral shapes for the 15, 17.5, and 20 mol % compositions shown in the inset of Figure 3c is striking, as it suggests that their dynamic environments are comparable.

In Figure 4, the key parameters characterizing dynamics and ion transport, as well as the relevant thermodynamic transitions, are plotted as functions of the composition of the ChCl/EG mixtures. Contrary to the common assumption that

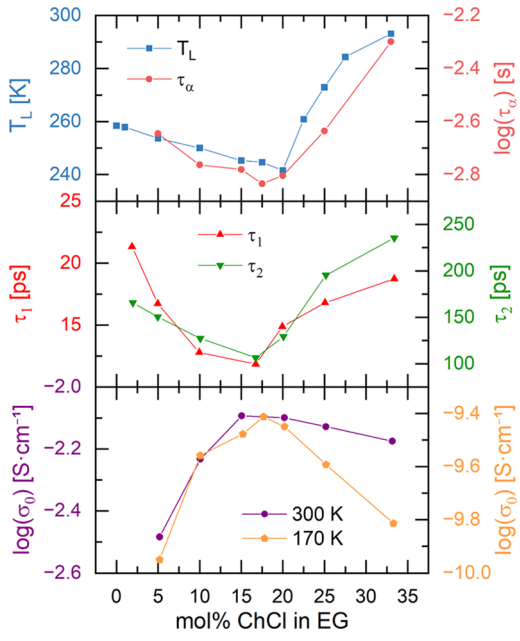

Figure 4. (a) Liquidus temperatures (blue squares) and structural relaxation rates from BDS at 170 K (pink circles) plotted versus mol % ChCl. (b) Relaxation time constants for the fast component τ_1 (red up triangles) and slow component τ_2 (green down triangles) from fs-TA kinetics of B30 in ethaline at room temperature plotted versus mol % ChCl. (c) DC ionic conductivities plotted versus mol % ChCl at 300 K (purple diamonds) and 170 K (orange pentagons). All three experimental quantities (panels a,b,c) suggest that the eutectic composition occurs in the 15−20 mol % range, depending on the technique employed.

the eutectic composition is at 33 mol % ChCl or a 1:2 molar ratio of ChCl to EG, it is evident that the composition with the lowest melting temperature is in the 15−20 mol % ChCl range. This result agrees with the solid−liquid equilibrium phase diagrams reported by Crespo et al. and Agieienko et al., which also shows that the lowest T_m occurs in this range for ChCl/EG mixtures.[25,40] Similarly, the structural relaxation rates from BDS at 170 K, plotted in Figure 4a, also show that the fastest dynamics occur in the 15−20 mol % ChCl range, consistent with the fs-TAS results in Figure 4b. To the best of our knowledge, this correlation between the eutectic composition and dynamics has not been previously reported. It is remarkable that the trend also holds for the other dielectric relaxations described earlier (Tables S3−S9).

The time constants from fs-TAS shown in Figure 4b indicate that the relaxation dynamics first speed up with increasing mol % of ChCl up to 16.67 mol % and then become slower as ChCl mol % composition continues to increase up to 33 mol %. This trend reveals a correlation between solvation dynamics and the thermodynamic transitions with the fastest dynamics at the eutectic composition. Consistent with the trends in the dynamics, Figure 4c shows that the dc ionic conductivity at 300 and 170 K are also enhanced in the 15−20 mol % ChCl range. The similarity of the dielectric spectral shapes in this concentration range shown in the inset of Figure 3c implies that the eutectic composition, as viewed from dynamics, could be regarded as a range rather than a single value. However, further DESs should be studied before a general conclusion can be made regarding this point. In any case, these results agree with the recent experimental and computational work by Zhang et al., also reporting a peak in the ionic conductivity at 20 mol % ChCl.[41] Although Zhang et al. attributed this observation to a balance between concentration and viscosity effects, the picture emerging in the current work implies that the ionic conductivity may simply be exhibiting a similar trend in the structural and ion dynamics.

Taken altogether, the current results suggest that the eutectic composition occurs in the 15−20 mol % ChCl range. The TL of 33 mol % ChCl in EG (previously reported eutectic composition) occurs at 293 K, which agrees with the first report by Abbott et al.[22] For simple liquids, Lindemann's criterion predicts a qualitative linear relationship between the glass transition (T_g) and melting temperatures.[42] Given that T_g is a manifestation of the primary structural relaxation, the enhancement of dynamics at the eutectic composition is intuitive. We now need to rationalize the apparent discrepancy between the reported zero-shear viscosity and the dynamics presented in the current work. In a report by Zhang et al., the zero-shear viscosity does not exhibit a similar trend with the concentration of the ChCl at the eutectic composition reported here.[41] Instead, the viscosity of ChCl/EG increases with increasing ChCl composition up to 33 mol %. We posit that slower mechanical relaxation modes exist beyond the primary structural dynamics that contribute to the overall viscosity of these mixtures. Indeed, the broadening of the dielectric spectra with increasing ChCl concentration observed in Figure 4, as well as the evidence of heterogeneities recently reported by Spittle et al., support this conjecture.[36] Overall, the data presented herein instead indicate that the 15−20 mol % ChCl composition range offers the best opportunities for faster orientational and solvation dynamics, in addition to improving the dc ionic conductivity. As such, these compositions should

https://doi.org/10.1021/jacsau.3c00420
JACS Au 2023, 3, 3024−3030

be relevant for applications requiring DESs to serve as media for solvation and transport.[43]

In conclusion, temperature-modulated differential scanning calorimetry, broadband dielectric spectroscopy, and femtosecond transient absorption spectroscopy are employed to investigate the impact of thermodynamic transitions on dynamics of mixtures of choline chloride and ethylene glycol across a wide range of compositions. It is shown that the eutectic composition range of the DES occurs at 15−20 mol % ChCl in EG, which correlates strongly with enhancement in the primary structural relaxation, solvation dynamics, and increases in the dc ionic conductivity. These results establish a link between the eutectic compositions and dynamics in the deep eutectic solvents.

EXPERIMENTAL METHODS

Sample Preparation

Ethylene glycol (EG) was purchased from ACROS Organics at ≥99% purity. Choline chloride (ChCl) was purchased from Sigma-Aldrich at ≥98% purity. Both ChCl and EG are known hygroscopic materials; therefore, additional steps were taken to control the water content. The ChCl was dried in a vacuum oven for at least 48 h at 70 °C, while EG was purchased dry and handled under nitrogen as received. Water contents of final compositions were screened with Karl Fischer titration using a target water content of ≤2 mg/g, with samples that exhibited greater water content being rejected and remade. Compositions were made by adding an appropriate amount of ChCl to EG, which were then stirred on a hot plate at 80 °C in a dry nitrogen atmosphere until fully liquid and homogeneous.[16] For fs-TAS experiments, Reichardt's dye (betaine-30) was added to the prepared mixtures to achieve an absorption of 0.5 at the excitation wavelength.

Differential Scanning Calorimetry

Differential scanning calorimetry (DSC) was employed to study thermodynamic transitions in the samples. DSC testing was performed by using a TA Instruments DSC 2500. The samples were prepared using hermetically sealed aluminum pans within an enclosed, nitrogen-purged glovebox to ensure zero mass transfer to the environment during sample preparation and testing. Tests were performed for each composition using constant heat flow heating and cooling cycles from −120 to 75 °C. Each composition was first annealed ≈20 °C above their respective melting points for 10 min and then thermodynamically cycled at a constant heating and cooling rate of 1 and 2 °C/min using both the temperature-modulated DSC (MDSC) scans for higher accuracy and standard heat−cool-heat cycling (HCH) to check for reversibility, hysteresis, and overall reproducibility of the measurements. Because T_L values represent the final temperature where the solid state can coexist in equilibrium with the liquid state, values are carefully determined graphically as the final temperature before the thermogram returns to the baseline (per labeled T_L values in Figure S1).

Steady-State UV−Vis Absorption Spectroscopy and Femtosecond Transient Absorption Spectroscopy

Steady-state UV−vis measurements were performed by using a Varian Cary 50 UV−vis spectrophotometer. Femtosecond transient absorption (fs-TA) measurements were carried out using a Clark MXR 2010 fs laser system that generates a fundamental output wavelength of 780 nm and a 100 fs laser pulse duration at a pulse repetition rate of 1 kHz. The laser beam was split to generate (i) a 390 nm pump pulse using a second harmonic generation crystal and (ii) a white-light continuum probe pulse by using a sapphire crystal. The probe light was delay-controlled by using a computer-controlled optical delay stage. All fs-TA measurements were carried out in 2 mm quartz cuvettes at room temperature. Pump power was chosen as low as possible, which still provided a reliable signal-to-noise ratio in order to avoid unnecessary photodamage of the probe molecule B30 dye at 40 mJ cm^{-2}. The fs-TA data were pulse chirp-corrected and globally fitted at selected monitoring wavelengths (550−600 nm) to biexponential decay functions, modeled by $TA(t,\lambda) = A_1\exp(-t/\tau_1) + A_2\exp(-t/\tau_2)$, where A_1 and A_2 are amplitude coefficients which combine to unity, t is the time, and τ_1 and τ_2 are the fitted time constants. Steady-state absorption spectra were taken before and after experiments to confirm that no photodegradation was indicated due to the laser spectroscopic experimentation.

Broadband Dielectric Spectroscopy

Broadband dielectric spectroscopy (BDS) measurements were performed in the frequency range 10^{-1} to 10^{7} Hz by using a Novocontrol High Resolution Dielectric Alpha Analyzer with a Quatro liquid nitrogen temperature control system with ±0.1K temperature stability. The BDS measurements were carried out using gold-plated brass electrodes, 20 mm in diameter, with Teflon spacers approximately 150 μm in thickness. Prior to measurement, the samples were annealed at 20 K above their respective melting points to establish that the spectra were not changing with time. The dielectric data were fit using a combination of a Debye function, Havriliak−Negami function, and a random barrier model. The three functions for the mixtures were necessary to account for contributions from the slow, structural α, and ion dynamics, respectively. These fit functions are outlined in the SI, as supporting eq 1. The fit results are shown in Tables S3−S9.

ASSOCIATED CONTENT

Supporting Information

The Supporting Information is available free of charge at https://pubs.acs.org/doi/10.1021/jacsau.3c00420.

Thermograms from DSC, fs-TAS relaxation dynamics, and BDS fitting parameters for all compositions (PDF)

AUTHOR INFORMATION

Corresponding Authors

Clemens Burda − *Department of Chemistry, Case Western Reserve University, Cleveland, Ohio 44106, United States;* orcid.org/0000-0002-7342-2840; Email: cxb77@case.edu

Joshua Sangoro − *Department of Chemical and Biomolecular Engineering, University of Tennessee, Knoxville, Tennessee 37996, United States; William G. Lowrie Department of Chemical and Biomolecular Engineering, The Ohio State University, Columbus, Ohio 43210, United States;* orcid.org/0000-0002-5483-9528; Email: sangoro.1@osu.edu

Authors

Stephanie Spittle − *Department of Chemical and Biomolecular Engineering, University of Tennessee, Knoxville, Tennessee 37996, United States*

Ibrahim Alfurayj − *Department of Chemistry, Case Western Reserve University, Cleveland, Ohio 44106, United States*

Benworth Bryce Hansen − *William G. Lowrie Department of Chemical and Biomolecular Engineering, The Ohio State University, Columbus, Ohio 43210, United States*

Kaylie Glynn − *William G. Lowrie Department of Chemical and Biomolecular Engineering, The Ohio State University, Columbus, Ohio 43210, United States*

William Brackett − *Department of Chemical and Biomolecular Engineering, University of Tennessee, Knoxville, Tennessee 37996, United States*

Rathiesh Pandian − *Department of Chemistry, Case Western Reserve University, Cleveland, Ohio 44106, United States*

https://doi.org/10.1021/jacsau.3c00420
JACS Au 2023, 3, 3024−3030

Complete contact information is available at:
https://pubs.acs.org/10.1021/jacsau.3c00420

Author Contributions

CRediT: **Stephanie Spittle** conceptualization, data acquisition, formal analysis, investigation, writing-original draft, writing-review & editing; **Ibrahim Alfurayj** formal analysis, investigation, methodology, writing-original draft, writing-review & editing; **Benworth B. Hansen** data acquisition, formal analysis, investigation, writing-original draft; **Kaylie Glynn** data curation, formal analysis, investigation, methodology, writing-original draft; **William Brackett** data acquisition, investigation; **Rathiesh Pandian** data acquisition, formal analysis, investigation; **Clemens Burda** conceptualization, formal analysis, funding acquisition, methodology, project administration, supervision, writing-original draft, writing-review & editing; **Joshua R. Sangoro** conceptualization, funding acquisition, investigation, methodology, project administration, overall supervision, writing-original draft, writing-review & editing.

Notes

The authors declare no competing financial interest.

■ ACKNOWLEDGMENTS

This work was supported as part of the Breakthrough Electrolytes for Energy Storage (BEES), an Energy Frontier Research Center funded by the US Department of Energy, Office of Science, Basic Energy Sciences under Award #: DE-SC0019409. This manuscript is partially based on the dissertation from the first author.

■ REFERENCES

(1) Wang, W.; Lee, D. J. Lignocellulosic Biomass Pretreatment by Deep Eutectic Solvents on Lignin Extraction and Saccharification Enhancement: A Review. *Bioresour. Technol.* **2021**, *339*, No. 125587, DOI: 10.1016/j.biortech.2021.125587.

(2) Kalhor, P.; Ghandi, K. Deep Eutectic Solvents as Catalysts for Upgrading Biomass. *Catalysts* **2021**, *11* (2), No. 178, DOI: 10.3390/catal11020178.

(3) Loow, Y.-L.; New, E. K.; Yang, G. H.; Ang, L. Y.; Foo, L. Y. W.; Wu, T. Y. Potential Use of Deep Eutectic Solvents to Facilitate Lignocellulosic Biomass Utilization and Conversion. *Cellulose* **2017**, *24* (9), 3591−3618.

(4) Palmelund, H.; Andersson, M. P.; Asgreen, C. J.; Boyd, B. J.; Rantanen, J.; Löbmann, K. Tailor-Made Solvents for Pharmaceutical Use? Experimental and Computational Approach for Determining Solubility in Deep Eutectic Solvents (DES). *Int. J. Pharm. X* **2019**, *1*, No. 100034.

(5) Emami, S.; Shayanfar, A. Deep Eutectic Solvents for Pharmaceutical Formulation and Drug Delivery Applications. *Pharm. Dev. Technol.* **2020**, *25* (7), 779−796.

(6) Aroso, I. M.; Silva, J. C.; Mano, F.; Ferreira, A. S. D.; Dionísio, M.; Sá-Nogueira, I.; Barreiros, S.; Reis, R. L.; Paiva, A.; Duarte, A. R. C. Dissolution Enhancement of Active Pharmaceutical Ingredients by Therapeutic Deep Eutectic Systems. *Eur. J. Pharm. Biopharm.* **2016**, *98*, 57−66.

(7) Ali, E.; Hadj-Kali, M. K.; Mulyono, S.; Alnashef, I. Analysis of Operating Conditions for CO2 Capturing Process Using Deep Eutectic Solvents. *Int. J. Greenhouse Gas Control* **2016**, *47*, 342−350.

(8) Luo, F.; Liu, X.; Chen, S.; Song, Y.; Yi, X.; Xue, C.; Sun, L.; Li, J. Comprehensive Evaluation of a Deep Eutectic Solvent Based CO2 Capture Process through Experiment and Simulation. *ACS Sustainable Chem. Eng.* **2021**, *9* (30), 10250−10265.

(9) Xu, Q.; Qin, L. Y.; Ji, Y. N.; Leung, P. K.; Su, H. N.; Qiao, F.; Yang, W. W.; Shah, A. A.; Li, H. M. A Deep Eutectic Solvent (DES) Electrolyte-Based Vanadium-Iron Redox Flow Battery Enabling Higher Specific Capacity and Improved Thermal Stability. *Electrochim. Acta* **2019**, *293*, 426−431.

(10) Zhang, C.; Ding, Y.; Zhang, L.; Wang, X.; Zhao, Y.; Zhang, X.; Yu, G. A Sustainable Redox-Flow Battery with an Aluminum-Based, Deep-Eutectic-Solvent Anolyte. *Angew. Chem.* **2017**, *129* (26), 7562−7567.

(11) Lloyd, D.; Vainikka, T.; Kontturi, K. The Development of an All Copper Hybrid Redox Flow Battery Using Deep Eutectic Solvents. *Electrochim. Acta* **2013**, *100*, 18−23.

(12) Wagle, D. V.; Zhao, H.; Baker, G. A. Deep Eutectic Solvents: Sustainable Media for Nanoscale and Functional Materials. *Acc. Chem. Res.* **2014**, *47* (8), 2299−2308.

(13) Florindo, C.; Oliveira, F. S.; Rebelo, L. P. N.; Fernandes, A. M.; Marrucho, I. M. Insights into the Synthesis and Properties of Deep Eutectic Solvents Based on Cholinium Chloride and Carboxylic Acids. *ACS Sustainable Chem. Eng.* **2014**, *2* (10), 2416−2425.

(14) Abbott, A. P.; Boothby, D.; Capper, G.; Davies, D. L.; Rasheed, R. K. Deep Eutectic Solvents Formed between Choline Chloride and Carboxylic Acids: Versatile Alternatives to Ionic Liquids. *J. Am. Chem. Soc.* **2004**, *126* (29), 9142−9147.

(15) Hansen, B. B.; Spittle, S.; Chen, B.; Poe, D.; Zhang, Y.; Klein, J. M.; Horton, A.; Adhikari, L.; Zelovich, T.; Doherty, B. W.; et al. Deep Eutectic Solvents: A Review of Fundamentals and Applications. *Chem. Rev.* **2021**, *121* (3), 1232−1285.

(16) Gurkan, B.; Squire, H.; Pentzer, E. Metal-Free Deep Eutectic Solvents: Preparation, Physical Properties, and Significance. *J. Phys. Chem. Lett.* **2019**, *10* (24), 7956−7964.

(17) Wazeer, I.; Hayyan, M.; Hadj-Kali, M. K. Deep Eutectic Solvents: Designer Fluids for Chemical Processes. *J. Chem. Technol. Biotechnol.* **2018**, *93* (4), 945−958.

(18) Guajardo, N.; Müller, C. R.; Schrebler, R.; Carlesi, C.; Domínguez De María, P. Deep Eutectic Solvents for Organocatalysis, Biotransformations, and Multistep Organocatalyst/Enzyme Combinations. *ChemCatChem* **2016**, *8* (6), 1020−1027.

(19) Song, Z.; Hu, X.; Wu, H.; Mei, M.; Linke, S.; Zhou, T.; Qi, Z.; Sundmacher, K. Systematic Screening of Deep Eutectic Solvents as Sustainable Separation Media Exemplified by the CO2Capture Process. *ACS Sustainable Chem. Eng.* **2020**, *8* (23), 8741−8751.

(20) Alizadeh, V.; Malberg, F.; Pádua, A. A. H.; Kirchner, B. Are There Magic Compositions in Deep Eutectic Solvents? Effects of Composition and Water Content in Choline Chloride/Ethylene Glycol from Ab Initio Molecular Dynamics. *J. Phys. Chem. B* **2020**, *124* (34), 7433−7443.

(21) Zhang, Q.; De Oliveira Vigier, K.; Royer, S.; Jérôme, F. Deep Eutectic Solvents: Syntheses, Properties and Applications. *Chem. Soc. Rev.* **2012**, *41* (21), 7108−7146.

(22) Abbott, A. P.; Capper, G.; Swain, B. G.; Wheeler, D. A. Electropolishing of Stainless Steel in an Ionic Liquid. *Trans. Inst. Met. Finish.* **2005**, *83* (1), 51−53.

(23) Ibrahim, R. K.; Hayyan, M.; AlSaadi, M. A.; Ibrahim, S.; Hayyan, A.; Hashim, M. A. Physical Properties of Ethylene Glycol-Based Deep Eutectic Solvents. *J. Mol. Liq.* **2019**, *276*, 794−800.

(24) García, G.; Aparicio, S.; Ullah, R.; Atilhan, M. Deep Eutectic Solvents: Physicochemical Properties and Gas Separation Applications. *Energy Fuels* **2015**, *29* (4), 2616−2644.

(25) Agieienko, V.; Buchner, R. Is Ethaline a Deep Eutectic Solvent? *Phys. Chem. Chem. Phys.* **2022**, *24* (9), 5265−5268.

(26) Smith, W. F.; Hashemi, J. *Foundation of Materials Science and Engineering*, 4th ed.; McGraw-Hill, 2006.

(27) Meng, X.; Ballerat-Busserolles, K.; Husson, P.; Andanson, J. M. Impact of Water on the Melting Temperature of Urea + Choline Chloride Deep Eutectic Solvent. *New J. Chem.* **2016**, *40* (5), 4492−4499.

(28) Yuan, L.; Clevers, S.; Couvrat, N.; Cartigny, Y.; Dupray, V.; Coquerel, G. Precise Urea/Water Eutectic Composition by Temperature-Resolved Second Harmonic Generation. *Chem. Eng. Technol.* **2016**, *39* (7), 1326−1332.

(29) Askeland, D. R.; Wright, W. J. *Essentials of Materials Science and Engineering*, 4th ed.; Cengage Learning, 2018.

(30) Reid, P. J.; Barbara, P. F. Dynamic Solvent Effect on Betaine-30 Electron-Transfer Kinetics in Alcohols. *J. Phys. Chem. A* **1995**, *99* (11), 3554−3565.
(31) Mente, S. R.; Maroncelli, M. Computer Simulations of the Solvatochromism of Betaine-30. *J. Phys. Chem. B* **1999**, *103* (36), 7704−7719.
(32) Alfurayj, I.; Fraenza, C. C.; Zhang, Y.; Pandian, R.; Spittle, S.; Hansen, B.; Dean, W.; Gurkan, B.; Savinell, R.; Greenbaum, S.; et al. Solvation Dynamics of Wet Ethaline: Water Is the Magic Component. *J. Phys. Chem. B* **2021**, *125* (31), 8888−8901.
(33) Levinger, N. E.; Johnson, A. E.; Walker, G. C.; Barbara, P. F. Specific Excitation of the Solvent Coordinate in the $S_3 \rightarrow S_1$ and $S_1 \rightarrow S_0$ Radiationless Decay of the Betaines. *Chem. Phys. Lett.* **1992**, *196* (1−2), 159−165.
(34) Kim, H.; Hwang, H.; Rossky, P. J. Quantum Simulation of Solution Phase Intramolecular Electron Transfer Rates in Betaine-30. *J. Phys. Chem. A* **2006**, *110* (39), 11223−11229.
(35) Horng, M. L.; Gardecki, J. A.; Papazyan, A.; Maroncelli, M. Subpicosecond Measurements of Polar Solvation Dynamics: Coumarin 153 Revisited. *J. Phys. Chem. A* **1995**, *99* (48), 17311−17337.
(36) Spittle, S.; Poe, D.; Doherty, B.; Kolodziej, C.; Heroux, L.; Haque, M. A.; Squire, H.; Cosby, T.; Zhang, Y.; Fraenza, C.; et al. Evolution of Microscopic Heterogeneity and Dynamics in Choline Chloride-Based Deep Eutectic Solvents. *Nat. Commun.* **2022**, *13* (1), No. 219, DOI: 10.1038/s41467-021-27842-z.
(37) Debye, P. *Polar Molecules*; Chemical Catalog Co., Inc.: New York, 1929.
(38) Griffin, P. J.; Cosby, T.; Holt, A. P.; Benson, R. S.; Sangoro, J. R. Charge Transport and Structural Dynamics in Carboxylic-Acid-Based Deep Eutectic Mixtures. *J. Phys. Chem. B* **2014**, *118* (31), 9378−9385.
(39) Zhang, Y.; Poe, D.; Heroux, L.; Squire, H.; Doherty, B. W.; Long, Z.; Dadmun, M.; Gurkan, B.; Tuckerman, M. E.; Maginn, E. J. Liquid Structure and Transport Properties of the Deep Eutectic Solvent Ethaline. *J. Phys. Chem. B* **2020**, *124* (25), 5251−5264.
(40) Crespo, E. A.; Silva, L. P.; Lloret, J. O.; Carvalho, P. J.; Vega, L. F.; Llovell, F.; Coutinho, J. A. P. A Methodology to Parameterize SAFT-Type Equations of State for Solid Precursors of Deep Eutectic Solvents: The Example of Cholinium Chloride. *Phys. Chem. Chem. Phys.* **2019**, *21* (27), 15046−15061.
(41) Zhang, Y.; Squire, H.; Gurkan, B.; Maginn, E. J. Refined Classical Force Field for Choline Chloride and Ethylene Glycol Mixtures over Wide Composition Range. *J. Chem. Eng. Data* **2022**, *67* (8), 1864−1871, DOI: 10.1021/acs.jced.1c00841.
(42) Lindemann, F. The Calculation of Molecular Natural Frequencies. *Phys. Zeitschrift* **1910**, *11*, 609−612.
(43) Spittle, S. Understanding Structure-Property Relationships in Deep Eutectic Solvents, PhD dissertation; University of Tennessee2022.

https://doi.org/10.1021/jacsau.3c00420
JACS Au 2023, 3, 3024−3030